The effect of concentration- and temperature-dependent dielectric constant on the activity coefficient of NaCl electrolyte solutions

Mónika Valiskó, and Dezső Boda*

Department of Physical Chemistry, University of Pannonia,
P.O. Box 158, H-8201 Veszprém, Hungary

(Dated: June 3, 2014)

Abstract

Our implicit-solvent model for the estimation of the excess chemical potential (or, equivalently, the activity coefficient) of electrolytes is based on using a dielectric constant that depends on the thermodynamic state, namely, the temperature and concentration of the electrolyte, $\epsilon(c,T)$. As a consequence, the excess chemical potential is split into two terms corresponding to ion-ion (II) and ion-water (IW) interactions. The II term is obtained from computer simulation using the Primitive Model of electrolytes, while the IW term is estimated from the Born treatment. In our previous work (Vincze *et al.*, J. Chem. Phys. 133, 154507, 2010), we showed that the nonmonotonic concentration dependence of the activity coefficient can be reproduced qualitatively with this II+IW model without using any adjustable parameter. The Pauling radii were used in calculation of the II term, while experimental solvation free energies were used in the calculation of the IW term. In this work, we analyze the effect of the parameters (dielectric constant, ionic radii, solvation free energy) on the concentration and temperature dependence of the mean activity coefficient of NaCl. We conclude that the II+IW model can explain the experimental behavior using a concentration-dependent dielectric constant and that we do not need the artificial concept of "solvated ionic radius" assumed by earlier studies.

PACS numbers: 02.70.-c, 02.70.Uu, 05.10.Ln

---

* Author to whom correspondence should be addressed: Electronic mail: boda@almos.vein.hu

I. INTRODUCTION

The Helmholtz free energy (G) cost of inserting an ion (of species i) into an electrolyte at a given pressure (p) and temperature (T) is called chemical potential and defined as

$$\mu_i = \left(\frac{\partial G}{\partial n_i} \right)_{p,T,n_{j,j\neq i}} , \tag{1}$$

where n_i is the quantity of the inserted matter (it can be a mole or just a single particle). In general, the free energy cost of bringing the particle from vacuum is considered; in the case of electrolytes, however, the reference point is the infinitely dilute electrolyte ($c \to 0$, where c is the concentration), e.g. the limiting case of pure solvent (usually, water). This means that the excess (EX) chemical potential is zero at infinite dilution

$$\lim_{c\to 0} \mu_i^{\mathrm{EX}}(c,T) = 0 \tag{2}$$

for any temperature, T. The excess chemical potential is defined through

$$\mu_i(c,T) = \mu_i^0(T) + kT \ln c_i + \mu_i^{\mathrm{EX}}(c,T), \tag{3}$$

where $\mu_i^0(T)$ is a reference chemical potential independent of the concentration (specifically, this is the chemical potential when $kT \ln c_i + \mu_i^{\mathrm{EX}} = 0$), k is Boltzmann's constant, and c_i is the concentration of species i (for NaCl, considered here, $c_+ = c_- = c$; subscripts $+$ and $-$ refer to cations and anions, respectively).

The central question of numerous theoretical and experimental studies is that how does the chemical potential depend on the concentration, c, and temperature, T, of the electrolyte. This question is reduced to the concentration and temperature dependence of the excess chemical potential or its multiplicative counterpart, the activity coefficient

$$\gamma_i(c,T) = \exp\left(\frac{\mu_i^{\mathrm{EX}}(c,T)}{kT} \right), \tag{4}$$

which is a traditional variable in physical chemistry.

Measuring the individual excess chemical potential, however, is not trivial. One cannot put a mole of ions into an electrolyte without also bringing the counterions. Determining the excess chemical potential from measurements of electrical potentials using electrochemical cells is also problematic due to the appearance of the liquid junction potential at the boundary of the two electrode. Whether it is just a practical problem or whether it undermines the whole concept of the individual excess chemical potential is still the subject of heated debates[1–8]. From our part, we consider μ_i^{EX} as a thermodynamically well-defined quantity that can be computed straightforwardly in computer simulations and theories (you can insert an individual ion into a simulation cell). Recent experimental papers suggest that it can be appropriately measured using ion-selective electrodes (see the papers of Wilczek-Vera *et al.*[2,4,9] and references therein) or an ionic liquid salt bridge[10].

In the present paper, however, we evade this minefield by considering the mean excess chemical potential defined as

$$\mu_{\pm}^{\mathrm{EX}}(c,T) = \frac{\mu_{+}^{\mathrm{EX}}(c,T) + \mu_{-}^{\mathrm{EX}}(c,T)}{2} \tag{5}$$

for a 1:1 electrolyte such as NaCl studied here. The mean activity coefficient is

$$\gamma_{\pm}(c,T) = \sqrt{\gamma_{+}(c,T)\gamma_{-}(c,T)} = \exp\left(\frac{\mu_{\pm}^{\mathrm{EX}}(c,T)}{kT}\right). \tag{6}$$

These quantities can be measured accurately[11].

The measurements show a nonmonotonic concentration dependence of $\mu_{\pm}^{\mathrm{EX}}(c)$ for a given temperature: increasing the concentration from zero it decreases from zero with a slope obeying the Debye-Hückel (DH)[12] limiting law, reaches a minimum at a large concentration, then increases again as the concentration approaches saturation. The basic reason of this phenomenon is that the interactions of the inserted ion with its surrounding change as more and more ion is added to the solution. The question (also addressed in this paper) is this: what is the nature of these interactions?

The classical theory is the DH theory that considers the ions as point charges and computes their interaction with the mean field of the ionic cloud around them. One major problem with this picture was understood from the beginning: ions are not point charges; they have finite size. Several modifications of the DH theory have been proposed that usually introduced various size parameters; their discussion can be found in standard books[11,13,14]. A recent approach by Fraenkel also uses the DH theory as a starting point[15–20].

The other problem with the DH theory lies in its mean-field nature. The solution of this problem arrived with modern statistical mechanical theories (including molecular simulations) and fast computers. The most famous of such theories (due to its relative simplicity and accuracy) is the Mean Spherical Approximation (MSA)[21]. The nonmonotonic behavior of the $\mu_{\pm}^{\mathrm{EX}}(c)$ function has been studied in several papers using this theory[22–31]. Computer simulations[32–36] and other theories[25,37–40] have also been used. We will discuss these works in the Discussion in detail.

The common aspect of these studies is that they use a well-specified microscopic model for the electrolyte. These models can be divided into two major classes on the basis of the modeling level of the solvent. Solvent molecules can be modeled explicitly (see Discussion) or implicitly by replacing them with their dielectric response. The implicit solvent approach is used in the Primitive Model (PM) of electrolytes, where the ions are represented as hard spheres with point charges in their centers (the charged hard sphere model). The interparticle potential acting between two ions of species i and j is given as

$$u_{ij}^{\mathrm{PM}}(r) = \begin{cases} \infty & \text{for } \; r < d_{ij} \\ \dfrac{z_i z_j e^2}{4\pi\epsilon_0\epsilon(c,T) r} & \text{for } \; r \geq d_{ij}, \end{cases} \tag{7}$$

where z_i is the valence of ionic species i, e is the elementary charge, ϵ_0 is the permittivity of vacuum, r is the distance between the ions, and d_{ij} is the distance of ions of species i and j at contact position. $\epsilon(c,T)$ is the dielectric constant of the surrounding medium, which is the whole electrolyte instead of just the solvent. Also, it depends on the thermodynamic state, (c,T). This is the main point of this paper. The statement that the PM potential is additive means that the Lorentz-Berthelot mixing rule is applied for the diameters:

$$d_{ij} = \frac{R_i + R_j}{2} \tag{8}$$

with R_i being the ionic radius. Computer simulations provide exact thermodynamic quantities apart from system-size errors and statistical noise, while theories always contain some kind of approximation.

There is, however, a common problem with the papers based on the PM[22–30,32–36,40] independent of the fact whether the authors used theory or simulation. The experimental trend of $\mu_{\pm}^{\mathrm{EX}}(c,T)$ at fixed T could be reproduced only if they used ions with very large radii. Depending on the method, model, and fitting procedure used by the authors (see Discussion), ionic diameters in the range 2.6-3.9 Å was proposed for Na^+ (as opposed to the 1.9 Å Pauling diameter) in order to reproduce the experimental behavior of $\mu_{\pm}^{\mathrm{EX}}(c,T)$ at 25 °C. In this picture, the excess chemical potential is just the result of ion-ion (II) interactions, because it assumes that the interaction of the ion with the water molecules (IW) remains unchanged as the concentration is increased. As a result, the IW term is constant for a given temperature and does not appear in μ_i^{EX} since it is the same at infinite dilution and at concentration c. Formally, the excess chemical potential can be divided into an electrostatic (EL) and a hard sphere (HS) part:

$$\mu_i^{\mathrm{EX}} = \mu_i^{\mathrm{II}} = \mu_i^{\mathrm{EL}} + \mu_i^{\mathrm{HS}} \tag{9}$$

corresponding to the Coulomb interaction and volume exclusion; the two parts of Eq. 7. The HS part was large enough to produce the upswing part of $\mu_{\pm}^{\mathrm{EX}}(c)$ only using large ions. The common explanation is that the large size of the ion models the strongly correlated hydration shell around the ion. The increased ionic radius was termed as "solvated radius".

In our previous study[41], we pointed out the major problems with this picture and provided an alternative approach. (1) Most importantly, the structure of the aqueous environment changes as more ions appear in the electrolyte. Ions exert a strong electric field that orients water molecules and alters their ability to screen the ions (dielectric saturation). This phenomenon manifests itself in a solid experimental fact: the static dielectric constant of the electrolyte decreases as concentration increases[42–53]. The dielectric constant, therefore, a physical quantity that depends on the thermodynamic state: $\epsilon = \epsilon(c, T)$. This must be taken into account in $\mu_{\pm}^{\mathrm{EX}}(c, T)$; ions get into a less favorable dielectric environment when they are brought from an infinitely dilute electrolyte ($\epsilon(c \to 0, T) = \epsilon_{\mathrm{w}}(T)$, where $\epsilon_{\mathrm{w}}(T)$ is the dielectric constant of water at temperature T) into a concentrated solution ($\epsilon(c, T) < \epsilon_{\mathrm{w}}(T)$). This practically corresponds to a change in the solvation free energy.

(2) The other problem lies in the concept of "solvated radius". The "solvated radius" makes sense in situations, where the hydration shell of the ion remains intact. The fact, for example, that the diffusion constant of smaller ions is larger is commonly explained by that the water molecules around the smaller ions are more strongly bound to the ion so the ion together with its hydration shell experiences stronger friction. This is a reasonable picture for this case, where other ions do not bother the hydration shell. In the calculation of the excess chemical potential, however, this is not the case. The dominant interaction term in μ_i^{EX} is the cation-anion interaction, which is attractive and, on average, stronger than the interaction between like ions. Cations and anions, on the other hand, can approach each other at contact position without a water molecule between them as shown by molecular dynamics (MD) simulations[54–61]. This is obvious because the cation-anion interaction is stronger than the ion-water interaction. To forbid the configurations of the contact positions

from the statistical sample of the phase space with an artificial "solvated radius" is a bad idea, because these are important configurations with large statistical weights (low energy).

Our solution to these problems is twofold. We suggested using (1) a concentration-dependent experimental dielectric constant and (2) Pauling radii of the "bare" ions. This approach requires the inclusion of the IW term in the excess chemical potential,

$$\mu_i^{\mathrm{EX}} = \mu_i^{\mathrm{II}} + \mu_i^{\mathrm{IW}} \tag{10}$$

because the interaction energy of an inserted ion changes (with respect to the infinitely dilute solution) not only because its interaction with the other ions changes, but also because its interaction with the surrounding solvent with a smaller dielectric constant changes (II+IW model). Our approach implies that the explanation of the nonmonotonic behavior of $\mu_i^{\mathrm{EX}}(c)$ is not only the balance of the EL and HS terms, but primarily the balance of the II and IW terms. Our model was able to reproduce the nonmonotonic behavior qualitatively without using any adjustable parameters. We use only experimentally well-established parameters in our model: Pauling radii, experimental dielectric constant, and experimental solvation energy.

In this paper, we further analyze the effects of these parameters on the example of NaCl. We show results for Shannon-Prewitt[62] ionic radii (in addition to the Pauling radii[63]) and for experimental dielectric constant data from various sources[64,65]. Additionally, we analyze the effect of temperature on the results and propose using experimental $\epsilon(c,T)$ data with the Pauling radii independent of temperature. These results also support our II+IW model.

The next section describes our methods to compute the II and IW terms. The Results section contains results for c-dependence at 25 °C and for T-dependence for different concentrations. The paper is concluded with a detailed Discussion of our results in relation to other studies.

II. CALCULATION OF THE II AND IW TERMS

A. Calculation of the II term

The II term has been calculated with the Adaptive Grand Canonical Monte Carlo (A-GCMC) simulation of Malasics and Boda[66,67]. The procedure works in the grand canonical ensemble, where the chemical potential is the independent variable instead of the concentration. To determine the chemical potentials, $\mu_i(c,T)$ that correspond to a prescribed concentration, c, at a given T requires an iterative procedure. The algorithm of the A-GCMC method is robust and provides not only the mean, but also the individual excess chemical potentials for a given state point (c,T). The underlying molecular model is the PM introduced in Eq. 7. The model requires establishing the molecular parameter, R_i, and the thermodynamic parameter, $\epsilon(c,T)$ (for NaCl, $z_+ = 1$ and $z_- = -1$). We emphasize that the radii of the "bare ions" (independent of c and T) were used for R_i and experimentally measured values were used for $\epsilon(c,T)$.

B. Calculation of the IW term

The IW term has been estimated with Born's treatment of solvation[68]. In this theory, the solvation free energy, ΔG_i^{s}, is assumed to be equal to the electrostatic energy change of the inversion of a spherical ion of radius R_i^{B} in the continuum of dielectric constant $\epsilon(c,T)$ and is given as

$$\Delta G_i^{\mathrm{s}}(c,T) = \frac{z_i^2 e^2}{8\pi\epsilon_0 R_i^{\mathrm{B}}(T)} \left(\frac{1}{\epsilon(c,T))} - 1 \right). \tag{11}$$

The IW part of the excess chemical potential is defined as the difference in the solvation free energy of the concentrated and dilute solutions:

$$\mu_i^{\mathrm{IW}}(c,T) = \Delta G_i^{\mathrm{s}}(c,T) - \Delta G_i^{\mathrm{s}}(T) = \frac{z_i^2 e^2}{8\pi\epsilon_0 R_i^{\mathrm{B}}(T)} \left(\frac{1}{\epsilon(c,T)} - \frac{1}{\epsilon_{\mathrm{w}}(T)} \right), \tag{12}$$

where $\Delta G_i^{\mathrm{s}}(T) = \Delta G_i^{\mathrm{s}}(c \to 0, T)$ is the experimental solvation (hydration) energy for temperature T. It is important to note that the radius R_i^{B} (the Born radius) does not have to be the same as R_i used in the calculation of the II terms (an unnecessary assumption made by Abbas *et al.*[35]). The Born radius is T-dependent. It is obtained from Eq. 11 by writing it up for the case of infinitely dilute electrolyte:

$$\Delta G_i^{\mathrm{s}}(T) = \frac{z_i^2 e^2}{8\pi\epsilon_0 R_i^{\mathrm{B}}(T)} \left(\frac{1}{\epsilon_{\mathrm{w}}(T)} - 1 \right). \tag{13}$$

Expressing $R_i^{\mathrm{B}}(T)$ from Eq. 13 and substituting into Eq. 12, we obtain an expression for the IW term that contains only experimental parameters:

$$\mu_i^{\mathrm{IW}}(c,T) = \Delta G_i^{\mathrm{s}}(T) \frac{\epsilon(c,T) - \epsilon_{\mathrm{w}}(T)}{\epsilon(c,T)\,(\epsilon_{\mathrm{w}}(T) - 1)}. \tag{14}$$

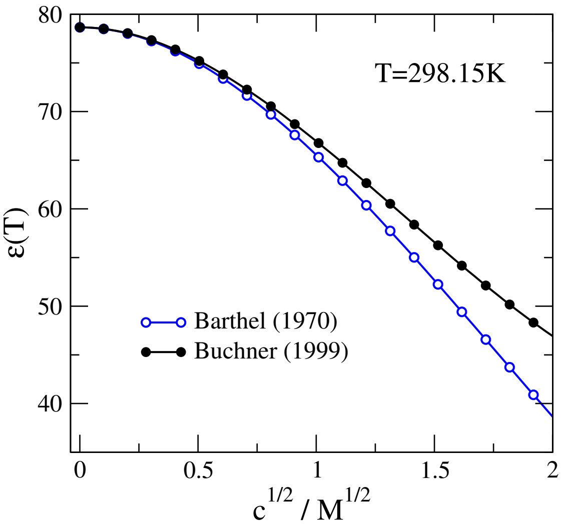

FIG. 1: Concentration dependence of the dielectric constant of NaCl electrolyte solution at $T = 298.15$ K from the measurements of Barthel *et al.*[64,69] (Eq. 15) and Buchner *et al.*[65] (Eq. 16).

Note that $\mu_i^{\mathrm{IW}}(c,T) > 0$ because $\epsilon(c,T) < \epsilon_{\mathrm{w}}(T)$ and $\Delta G_i^{\mathrm{s}}(T) < 0$. This equation describes the $\epsilon(c,T)$-dependence of the IW term.

III. RESULTS

All that remains is to find experimentally well-established data for R_i, $\Delta G_i^{\mathrm{s}}(T)$, and $\epsilon(c,T)$. We show results for the concentration-dependence at $T = 298.15$ K, so functions without T in the argument refer to this temperature, for example, $\mu_i^{\mathrm{EX}}(c)$ and $\epsilon(c)$. Also, functions without c in the argument refer to infinite dilution, for example, $\epsilon_{\mathrm{w}}(T)$ and $\Delta G_i^{\mathrm{s}}(T)$.

A. Concentration dependence

1. *Effect of solvation free energy*

The solvation free energies for $T = 298.15$ K found in different sources[11,13,14,70,71] are very similar and have little effect on the calculated $\mu_i^{\mathrm{IW}}(c)$ values compared to the errors introduced by different choices of R_i and $\epsilon(c)$. Therefore, we used the values reported by Fawcett[14,70]: $\Delta G_{\mathrm{Na}^+}^{\mathrm{s}} = -424\ \mathrm{kJ\,mol^{-1}}$ and $\Delta G_{\mathrm{Cl}^-}^{\mathrm{s}} = -304\ \mathrm{kJ\,mol^{-1}}$. The Born radii corresponding to these free energies are $R_{\mathrm{Na}^+}^{\mathrm{B}} = 1.62$ Å and $R_{\mathrm{Cl}^-}^{\mathrm{B}} = 2.26$ Å. For comparison, the Pauling radii are $R_{\mathrm{Na}^+} = 0.95$ Å and $R_{\mathrm{Cl}^-} = 1.81$ Å.

2. Effect of dielectric constant

In our previous work[41], we used the experimental data of Barthel *et al.*[64,69] from the 1970s fitted by

$$\epsilon_{1970}(c) = 78.45 - 16.2\,c + 3.1\,c^{3/2}. \tag{15}$$

Later, we came across the paper of Buchner *et al.*[65] from 1999, who performed impedance measurements for lower frequencies (from 200 MHz as opposed to 1 GHz in the case of Barthel *et al.*). Their extrapolations to zero frequency for the static dielectric constant, therefore, are more reliable. Their data fitted with

$$\epsilon_{1999}(c) = 78.45 - 15.45\,c + 3.76\,c^{3/2} \tag{16}$$

agreed with the data of Nörtemann *et al.*[72] well. The $\epsilon(c)$ data obtained from the two measurements are seen in Fig. 1. The data of Buchner *et al.* show weaker concentration dependence.

Figure 2a shows the normalized chemical potential curves, $\mu_{\pm}^{\mathrm{EX}}(c)/kT = \ln \gamma_{\pm}(c)$, and the II and IW components as obtained using either the $\epsilon_{1970}(c)$ (Eq. 15) or $\epsilon_{1999}(c)$ (Eq. 16) dielectric constant functions. The data are plotted as functions of $c^{1/2}$. The Pauling radii were used in the simulations for the II term.

As c increases, the II term decreases steeply towards more negative values monotonically. This decrease is due to two effects. (1) As the concentration increases, the cations and the anions are closer to each other on average, so the average attractive interaction between them is deeper. (2) As the concentration increases, the dielectric constant decreases (see Fig. 1), so the Coulomb interaction between cations and anions is less screened (we divide by a smaller number in Eq. 7). Both of these effects decrease the ES part (see Eq. 9) with increasing c. Using the Pauling radii, the HS part is not able to balance this continuous decrease.

There is, however, the IW part that is positive and increases with increasing concentration. This increase is due to the increasing solvation penalty that one pays during bringing an ion from the infinitely dilute solution ($\epsilon_w = 78.45$) to the concentrated solution ($\epsilon(c)$).

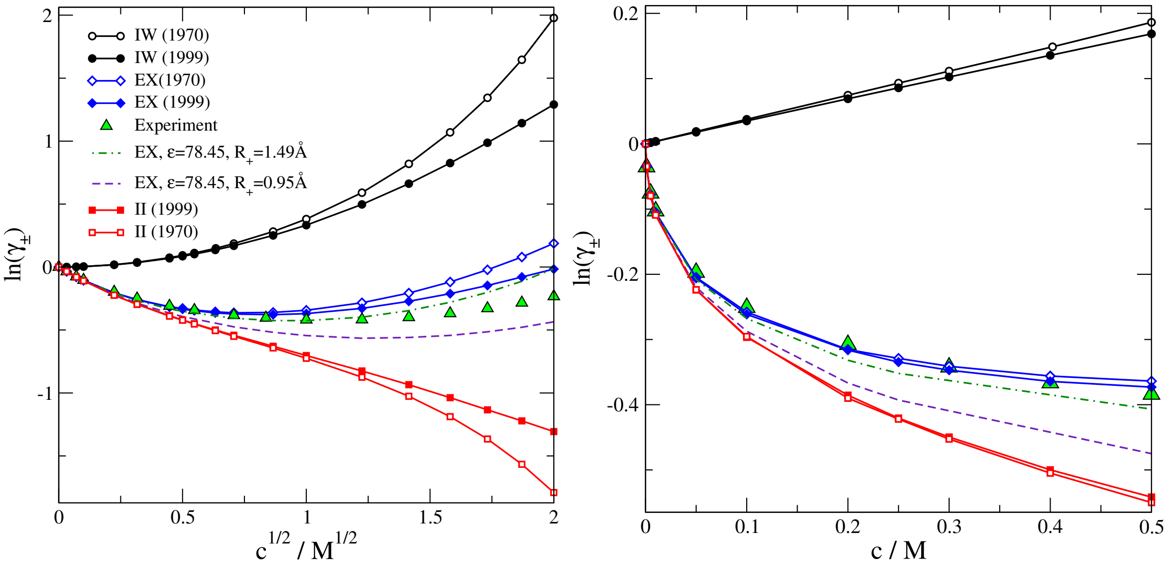

FIG. 2: The effect of different choices of the dielectric constant on the mean excess chemical potential (the IW, EX, and II terms are shown, from top to bottom) of NaCl at $T = 298.15$ K. Results using the dielectric constant of Barthel *et al.*[64,69] from 1970 (Eq. 15) and Buchner *et al.*[65] from 1999 (Eq. 16) are shown against experimental data[11]. The Pauling radii were used in these calculations. Results for fixed (concentration-independent) dielectric constant ($\epsilon = 78.45$) are also shown for two different Na$^+$ radii (see the text). Panel a plots the data as functions of $c^{1/2}$, while panel b focuses on the data for low concentrations ($c \leq 0.5$ M) as a function of c.

The sum of the II and IW components (EX curves in Fig. 2) is nonmonotonic. The agreement with the experimental data is quantitative for relatively low concentrations ($c < 0.5$ M, Fig. 2b), while it is qualitative for larger concentrations (Fig. 2a). We judge the agreement satisfactory given that we do not use adjustable parameters in our model. The agreement is better with the newer dielectric constant values.

Figure 2 also shows the curves for fixed (concentration-independent) dielectric constant, $\epsilon = 78.45$, for two sets of ionic radii. In both cases, the Cl$^-$ radius was fixed at the Pauling value (1.81 Å). The cation radius was the Pauling radius in one case (0.95 Å) and a fitted radius (1.49 Å) in the other case (the fit was based on that the simulation reproduced the experimental value for $c = 1$ M). The curve using the Pauling radius, as expected, underestimates the experimental curve. Figure 2a implies that it underestimates the experimental curve in about the same degree as our II+IW theory (using the Buchner dielectric constants)

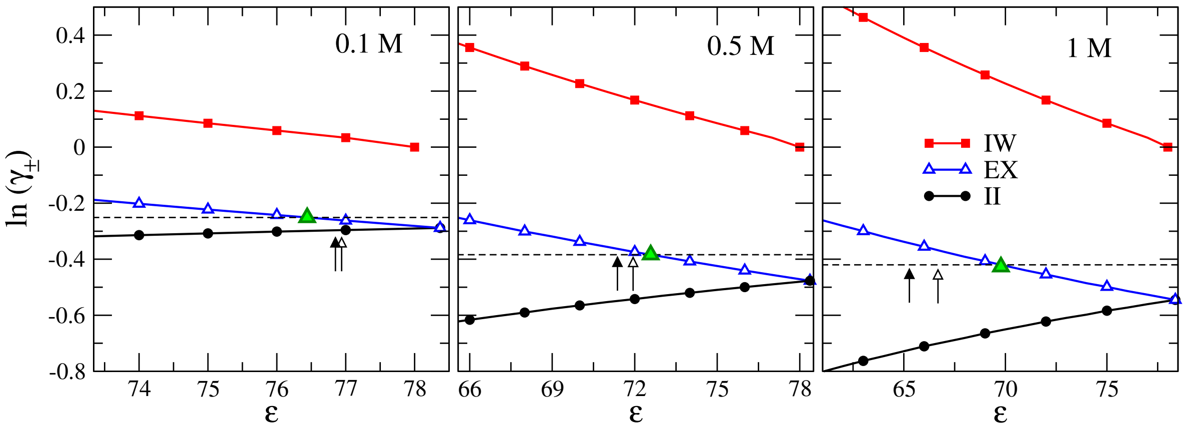

FIG. 3: The effect of dielectric constant by plotting the IW, EX, and II terms for three different concentrations (panels a-c). Experimental data are indicated by horizontal dashed lines. The crosspoints of these experimental lines and the computed EX curves are indicated by green triangles. The experimental dielectric constant values that correspond to the given concentrations are indicated by arrows (filled arrows: Barthel *et al.*[64,69], open arrows: Buchner *et al.*[65]).

overestimates it. This might give the impression that the two approaches are equally good (or equally bad). Figure 2b, however, shows that the constant-ϵ approach with $R_+ = 0.95$ Å (dashed line) fails at low concentrations, while our approach works very well. The other constant-ϵ simulation with $R_+ = 1.49$ Å (dot-dashed line) overestimates the experimental data for $c > 1$ M (Fig. 2a), while underestimates them for $c < 1$ M (Fig. 2b).

These results imply that the constant-ϵ approach cannot reproduce the trend of the experimental curve. We can fit the ionic radii at whatever concentrations, it would not work well at other concentrations. The II+IW approach, on the other hand, works properly in the low-concentration range without any adjustable parameter. This agreement is especially rewarding (Fig. 2b), because any model should work well in the "easy" cases (low concentrations) and have problems in the "hard" cases (high concentrations). We feel that the excellent agreement with experiments in the low concentration range is an important support for our model.

We can draw conclusions about the effect of the dielectric constant if we plot the curves as functions of ϵ. Figure 3 shows the II, IW, and EX curves for three fixed concentrations ($c = 0.1$, 0.5, and 1 M in Figs. 3a, b, and c, respectively) as functions of ϵ. The dielectric constant values used in these calculations do not necessarily correspond to experimental

	Na^+-Na^+	Cl^--Cl^-	Na^+-Cl^-
Pauling[63]	1.9	3.62	2.76
Shannon-Prewitt[62]	2.32	3.34	2.83
MD-based[54,59]	3.0	4.0	2.5
Fraenkel[15]	1.94	3.62	3.44

TABLE I: Ion-ion contact distances (d_{ij}) in Å for NaCl for different cases (see the text). For the Pauling and the Shannon-Prewitt radii, the PM potential (Eq. 7) is additive (see Eq. 8)

data. The experimental values (Eqs. 15 and 16) are indicated with arrows in the figure. The horizontal dashed line shows the experimental value for $\ln \gamma_{\pm}$ for the given concentration.

As ϵ decreases, the II term decreases, while the IW term increases as discussed above. Their sum (the EX term) is equal to the experimental value at ϵ that is quite close to the experimental $\epsilon_{1999}(c)$ data. The crosspoints of the EX and experimental curves are indicated with green triangles. The values are 76.44, 72.58, and 69.78 for $c = 0.1$, 0.5, and 1 M, respectively. The corresponding experimental values by Buchner *et al.* (the open arrows) are 77.02, 72.05, and 66.76, for the given concentrations, respectively.

3. *Effect of ionic radius*

The choice of the values proposed by Pauling[63] for the radii, R_i, of the "bare ions" in the calculation of the II term using the PM potential (Eqs. 7-8) is a natural one. There are, however, other choices. The Shannon-Prewitt radii[62], for example, are slightly different from the Pauling radii (see Table I).

We performed calculations for the II terms using both the Pauling and the Shannon-Prewitt radii in Eqs. 7-8. The results are seen in Fig. 4. Only the excess chemical potentials (EX) are shown. The difference between the results from the Pauling and the Shannon-Prewitt radii is minor. The explanation is that the d_{+-} (the distance of closest approach of the cation and the anions) value is similar for the two sets of radii (2.76 Å vs. 2.83 Å, see Table I). Although the Na^+ and Cl^- radii are quite different, their sums are close in the two cases. The d_{+-} distance, on the other hand, is a dominant parameter in the calculation of the II term, because it determines the distance of closest approach for the Na^+-Cl^- pair.

Fraenkel[15] developed a theory based on the DH treatment called "smaller-ion shell" (SiS)

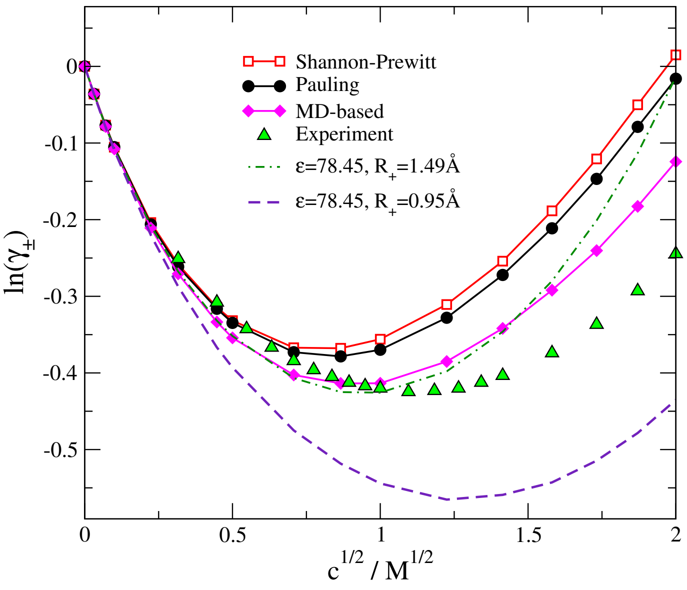

FIG. 4: The effect of different choices for the ionic radii used in the simulation of the II term on the mean excess chemical potential (EX term) of NaCl at $T = 298.15$ K. The dielectric constant of Buchner *et al.*[65] (Eq. 16) were used in these calculations. Results using the Pauling[63] and the Shannon-Prewitt[62] radii are plotted. The curve indicated as "MD-based" was computed using ionic radii deduced from RDFs obtained by MD simulations (see the text, Table I, and the arrows in Fig. 5). Results for fixed (concentration-independent) dielectric constant ($\epsilon = 78.45$) are also shown for two different Na^+ radii (see the text).

theory. He proposed that the distance of the ionic cloud from the central ion does not have to be the sum of the ionic radii. In the terminology of our PM, this means that d_{ij} is not necessarily equal to $R_i + R_j$, namely, the interionic potential does not have to satisfy the Lorentz-Berthelot mixing rule. In the case of implicit solvent electrolytes, this is a reasonable assumption, because water molecules play a role in the distances in which the ions tend to approach each other. In other words, water molecules influence the radial distribution functions (RDF) of the various ion pairs.

Inspired by the suggestion of Fraenkel, we looked up several MD simulations for NaCl electrolytes based on explicit water models[54–61]. The RDFs from two of them[54,59] are shown in Fig. 5. The $d_{ij} = R_i + R_j$ values according to the Pauling radii are indicated with vertical blue lines. The figure shows that the d_{++} contact value from MD simulations is larger than the Pauling diameter implying that water molecules of the hydration shells of Na^+ ions tend

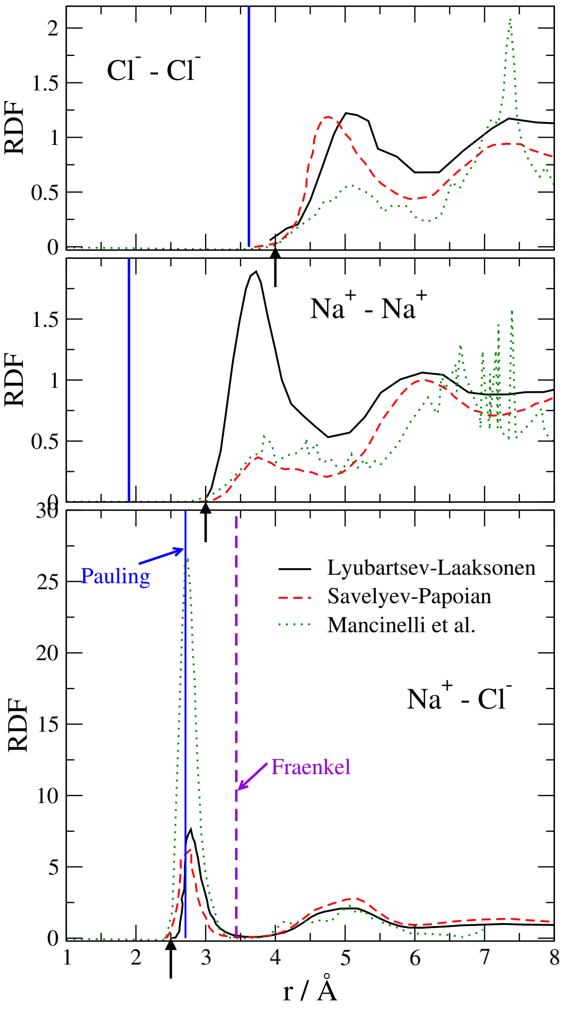

FIG. 5: Radial distribution functions for Na^+–Na^+, Na^+–Cl^-, and Cl^-–Cl^- pairs from MD simulations of Lyubartsev and Laaksonen[54] (for 0.8 M) and Saveliev and Papoian[59] (for 0.5 M). Experimental curves from Mancinelli *et al.*[73,74] are also shown for 0.7 M. Vertical solid lines indicate the Pauling values ($d_{ij} = R_i + R_j$), while vertical dashed line indicates the d_{+-} value obtained by Fraenkel[15]. Arrows indicate the d_{ij} values chosen to simulate the II term.

to prevent Na^+ ions from approaching each other at contact. In the Cl^--Cl^- case, on the other hand, these two values are similar due to the weaker repulsion between Cl^- ions and the fact that the hydration shell of Cl^- ions is less stable than the hydration shell of Na^+ ions.

The pair of counter-ions, on the other hand, can approach each other closer than the sum of Pauling radii due to the strong attraction between them. Seemingly, water molecules cannot prevent contact position. This result itself questions the idea of "solvated ionic radius". Positions of Na^+-Cl^- pairs close to contact form an essential part of the configurational space and must be part of the statistical sample.

Interestingly, Fraenkel found[15] that the SiS theory reproduces the experimental data if the d_{+-} value of unlike pairs is 3.44 Å, namely, it is larger than the sum of the Pauling radii, 2.78 Å (indicated by a vertical dashed line in the bottom panel of Fig. 5). This contradicts the MD results. This contradiction was discussed in our debate with Fraenkel in the J. Chem. Phys.[16,75].

The idea of the non-additive PM potential ($d_{+-} \neq R_+ + R_-$), however, inspired us to deduce d_{ij} values from the RDF curves of Fig. 5. The chosen values (Table I) correspond to the distances where the RDFs go to zero (indicated by arrows in Fig. 5). Because these RDFs are obtained from MD simulations with explicit water, we can introduce information into our coarse-grained model that has been obtained from calculations on a more refined, atomistic level. These MD results, furthermore, agree with experimental data[73,74] quite well as far as the contact distances of ions are concerned (see Fig. 5). This is an example of multi-scale modeling, where computations on the modeling levels of varying resolutions can support and complement each other.

The results for the EX curves obtained from the A-GCMC simulations using these d_{ij} values are shown in Fig. 4 with magenta diamonds. Interestingly, these calculations provide better agreement with experiments at large concentrations, but ruin the good agreement at low concentrations. Drawing more far-reaching conclusion would require calculations for more electrolytes beyond NaCl.

B. Temperature dependence

The temperature dependence of the activity coefficient was not considered in our previous paper[41]; it is computed on the basis of the II+IW model for the first time in this work. In order to perform these calculations, we need the temperature dependence of the physical quantities $\Delta G_i^{\mathrm{s}}(T)$ and $\epsilon(c,T)$ (the Pauling radii are used to simulate the II term in this section).

1. *Effect of solvation free energy*

As far as the solvation free energy is concerned, the temperature dependence is very small. Actual experimental data[47,49] indicate a small change of a few $\mathrm{kJ\,mol^{-1}}$ in the temperature range $273.15 - 373.15$ K considered in this work. Simplistic calculations with the approximation $\Delta G_i^{\mathrm{s}}(T) = \Delta G_i^{\mathrm{s}}(298.15) - S_i^{\mathrm{s}}(298.15)(T - 298.15)$ also yield a small change that does not influence our results for $\mu_{\pm}^{\mathrm{EX}}(c,T)$ considerably (data not shown). Therefore, we present results using the ΔG_i^{s} values for $T = 298.15$ K (see section III A 1)

2. *Effect of dielectric constant*

As far as the dielectric constant is concerned, the effect of temperature can be introduced into our calculations in three different ways.

- We fix the dielectric constant at the value $\epsilon = 78.45$ (the value for water at room temperature; filled square in Fig. 6). The IW term is zero in this case. The II term is influenced by temperature through the acceptance probabilities of the MC moves.
- We use the T-dependent dielectric constant of water, $\epsilon_{\mathrm{w}}(T)$, for which solid, reliable data are available[11]. We assume that the dielectric constant does not depend on concentration (open squares in Fig. 6). The IW term is zero in this case too. The II term is influenced not only by T in the acceptance probabilities of the MC moves, but also by the changing $\epsilon_{\mathrm{w}}(T)$ in the denominator of Eq. 7.
- We can take into account the dependence of the dielectric constant on both temperature and concentration, $\epsilon(c,T)$. Experimental data for $\epsilon(c,T)$, however, are very scarce. For concentrated electrolytes, we found data in the work of Helgeson and Flowers[48] (Fig. 10 of their paper). Data for the concentration $c = 1$ M are shown in Fig. 6 from two sources: Pottel *et al.*[46,76] and Hasted and Roderick[43]. The data of Pottel *et al.*[46,76] are the newest and they agree with the data of Buchner *et al.*[65] for 298.15 K (indicated with green triangles). Therefore, we use the measurements of Pottel *et al.* as the basis of our interpolation in the concentration range $0 \leq c \leq 1$ M and temperature range $273.15 \leq T \leq 373.15$.

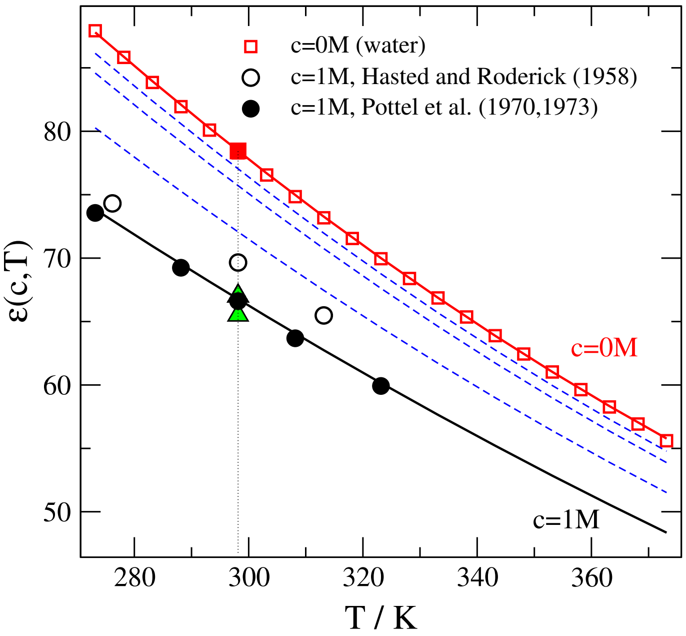

FIG. 6: Temperature dependence of the dielectric constant of NaCl solutions. Symbols denote experimental points, while curves denote interpolations/extrapolations obtained from Eq. 17. Open squares denote experimental data for water[11]. For $c = 1$ M, the data of Pottel *et al.*[46,76] (filled circles) and Hasted and Roderick[43] (open circles) are shown. The triangles show the data of Barthel *et al.*[64,69] and Buchner *et al.*[65] for $c = 1$ M and $T = 298.15$ K. The blue dashed lines are fits for $c = 0.1$, 0.2, and 0.5 M (from top to bottom) as described in the text.

In Figure 6, the experimental data are shown as symbols, while the curves represent interpolations/extrapolations. We fitted second order polynomials to the experimental data for $c \to 0$ and $c = 1$ M using the following equation

$$\epsilon(c,T) = \epsilon_{1999}(c) + \alpha(c)\,(T - 298.15) + \beta(c)\,(T - 298.15)^2. \tag{17}$$

We accepted the data of Buchner *et al.*[65] (Eq. 16) for $T = 298.15$ K. The coefficients are $\alpha(0) = -0.35596$ T^{-1}, $\alpha(1) = -0.27359$ T^{-1}, $\beta(0) = 0.00071466$ T^{-2}, and $\beta(1) = 0.00037564$ T^{-2}. The data of Pottel *et al.*[46,76] are available for temperatures below 323.15 K, so the fit is an extrapolation above this temperature. We obtained the $\alpha(c)$ and $\beta(c)$ values between 0 and 1 M with a linear fit. Our fitted functions are plotted for $c = 0.1$, 0.2, and 0.5 M as dashed blue lines in Fig. 6.

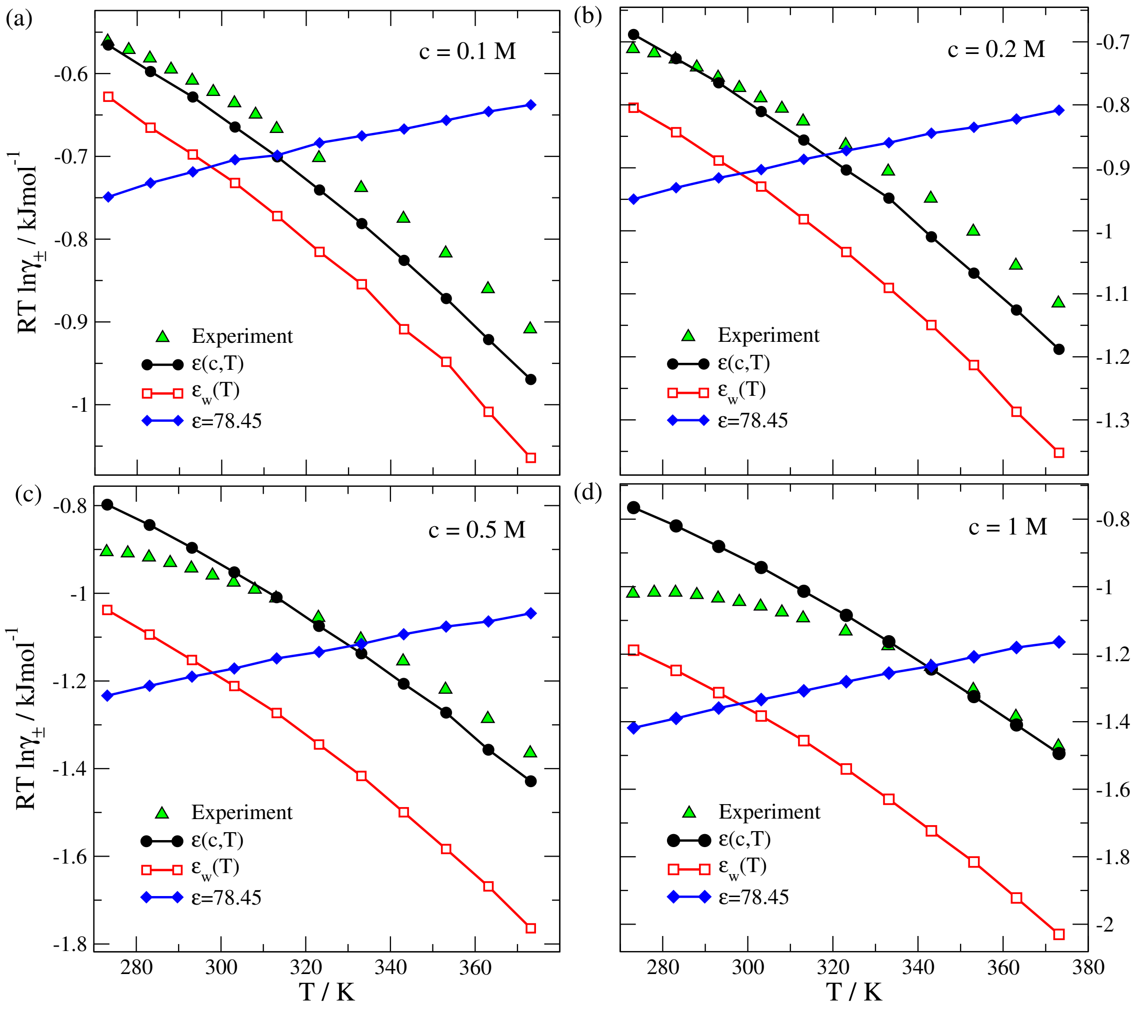

FIG. 7: Temperature dependence of the mean excess chemical potential $\mu_{\pm}^{\mathrm{EX}} = RT \ln \gamma_{\pm}$ for different concentrations compared to experimental data[11]. Different curves are obtained from different calculations by assuming different concentration and/or temperature dependence for the dielectric constant (for details, see the text).

We performed calculations with the II+IW model for these three cases and show the corresponding results in Fig. 7. The excess chemical potentials, $\mu_{\pm}^{\mathrm{EX}} = RT \ln \gamma_{\pm}$ are plotted as functions of the temperature for different concentrations (panels a-d), where $R = 8.314$ J/mol K is the gas constant. We show the full excess chemical potential (not only the $\ln \gamma_{\pm}$ term normalized by RT) because this quantity contains the effect of temperature both in the RT factor and in the $\ln \gamma_{\pm}$ term (resulting in smoother functions that are more relevant from a practical point of view). Note that the experimental data refer to molalities

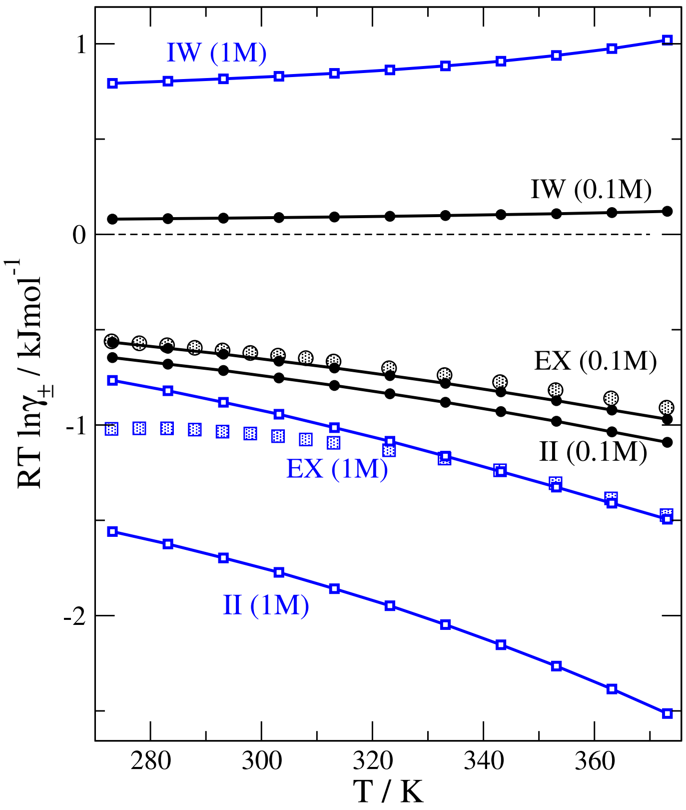

FIG. 8: Figures 7a and d replotted for concentrations $c = 0.1$ and 1 M also showing the II and IW terms. Only the results obtained from the $\epsilon(c, T)$ calculations are shown. Symbols without lines are experimental data[11].

(the difference is small in this concentration range; molality $m = 1$ mol/kg corresponds to molarity $c = 0.98036$ M, for example).

The figure shows that the assumption of fixed (both c- and T-independent) dielectric constant leads to qualitatively wrong results; the excess chemical potential increases with increasing temperature in contrast to the experimental trend. The other two models, where the T-dependence of the dielectric constant is assumed, on the other hand, reproduce the qualitative experimental behavior properly. This result already shows that the dependence of the dielectric constant of at least one of the thermodynamic parameters (T) must be taken into account. The agreement is qualitative for the $\epsilon_{\mathrm{w}}(T)$ case, where the c-dependence of the dielectric constant is ignored. The curves using the full $\epsilon(c, T)$ data in the studied (c, T) range, on the other hand, can reproduce the experimental data quite well. Deviations occur for larger concentrations ($c \geq 0.5$ M)) and smaller temperatures ($T < 320$ K). These deviations probably indicate that the applicability of the implicit water model becomes limited in this concentration and temperature range. We can conclude, therefore, that also taking the other parameter (c) into account is advantageous.

Figure 8 also shows the IW and II terms for $c = 0.1$ and 1 M in order to assess the behavior of the II+IW model. We show the data computed from the interpolations for $\epsilon(c, T)$ only. Disagreement with experiments for $c = 1$ M and lower temperatures, in our opinion, indicates the limitations of the implicit water modeling level rather than inadequacies in the measured dielectric constants. The agreement at larger temperatures shows that the II+IW model works better where thermal motion dominates over the structural effects of the water molecules in the hydration shells. At lower temperatures, on the contrary, consideration of such structural effects through explicit water models can be useful. Another limitation of the implicit-solvent model (the effect of cation radius in the LiCl–CsCl series) was analyzed in our previous work[41] and the need for explicit water simulations was pointed out.

We emphasize again that the II+IW theory provides these results using only experimental input without using adjustable parameters. The experimental input for the T-dependent dielectric constant is limited; more data are needed for a more elaborated study based on the II+IW model. The conclusion that the results for the T-dependence also support the II+IW model, however, can be drawn even from these limited set of calculations.

IV. DISCUSSION

The main strength of our model, in our opinion, that it gives a qualitative explanation for the nonmonotonic concentration dependence of the activity coefficient of electrolytes without using any adjustable parameter. It reproduces the temperature dependence too. All the parameters we used in our work were either microscopic parameters of the PM model (ion charge and radius), or thermodynamic parameters that have well-defined values in the thermodynamic state point. Our thermodynamic state point is defined by the temperature, T, and concentration, c. The pressure does not appear explicitly in our calculations; its effect enters our formalism implicitly through the solvation free energy and the dielectric constant.

Our agenda is that if a macroscopic physical quantity depends on the state point, it should be reflected in the calculations. In particular, it is an experimental fact that the dielectric

Paper	ϵ	d_+	d_-
Triolo *et al.* (1976)[22]	78	2.59	3.6
Triolo *et al.* (1977)[23]	$78.38(1.152+0.0048c)$	2.59	3.6
Triolo *et al.* (1977)[23]	$92.6(1+0.22c)$	1.9	3.6
Triolo *et al.* (1978)[24]	78	$3.33(1-0.079c)$	3.6
Simonin *et al.* (1996)[26]	$78.38/(1+0.0818c)$	$3.9-0.0303c$	$3.9-0.0303c$
Simonin *et al.* (1996)[26]	$78.38/(1+0.0816c)$	$3.76-0.0153c$	3.6
Fawcett *et al.* (1996)[28]	$78.45-19c+5c^{3/2}$	3.88	3.88

TABLE II: Fits of the dielectric constants and ionic radii obtained by various workers.

constant depends on the concentration of the electrolyte in addition to the temperature. The idea of using a concentration-dependent dielectric constant in calculations for the activity coefficients is not new. At the beginning, it was adjusted (together or without the ionic radii) so that the MSA calculations reproduce the experimental data. A few classical works for MSA calculations in the PM framework are collected in Table II. The authors either used the Pauling diameter for Cl^-[22–24,26] or used the same diameter for the two ions[26,28] (Restricted Primitive Model, RPM). The diameter of Na^+ was adjusted and it was either constant[22,23,28] or concentration dependent[23,24,26]. The dielectric constant was either fixed[22,24] or adjusted (concentration dependent)[23,26]. A concentration- and temperature-dependent dielectric constant was used by López-Pérez *et al.*[31], but $\epsilon(c,T)$ was an adjustable parameter in their MSA study.

These fits sometimes gave peculiar results. For example, the dielectric constant of water ($c = 0$ M) is larger than 90 and increases with concentration in the work of Triolo *et al.*[23]. Furthermore, the concept of a concentration-dependent ionic diameter was also used in some of these studies[24,26]. López-Pérez *et al.*[31] went further; they studied temperature and concentration dependence using MSA and assumed concentration- and temperature-dependent cation radius. We prefer if the thermodynamic state (concentration) enters the calculation through macroscopic parameters (ϵ) rather than through microscopic parameters. In any case, the IW term was ignored in these calculations.

The experimentally motivated concentration-dependent dielectric constant was proposed by Fawcett *et al.*[28–30]. They used the measurements of Barthel *et al.*[64,69] and the MSA theory of Simonin *et al.*[26,27] in the framework of the RPM, but the IW term was ignored by them too. In other works, they built ionic association into their model[29,30].

There are two notable exceptions where the IW term was taken into account. Inchekel *et al.*[40] applied an extension to the Cubic Plus Association equation of state for electrolytes using several free energy terms with many adjustable parameters. They found that the two dominant terms are those corresponding to our II and IW terms, although computed differently. They used MSA for the II term, while they interpreted the Born term (Eq. 11) as a Gibbs free energy and obtained the chemical potential by differentiation. The relation of the II and IW terms (II large negative, while IW large positive), however, is very similar to our results (see Fig. 1 of their paper).

Abbas *et al.*[35] used practically the same formalism for the IW term that we used. To obtain the II term, they applied canonical MC simulations with Widom's particle insertion method[77] modified by Svensson and Woodward[78]. Their procedure, however, differed from ours in two crucial aspects. (1) They used the same radius for both ions as an adjustable parameter. (2) They used the same radius in the Born-term and in the calculations for the II term ($R_i = R_i^{\mathrm{B}}$). They did not decouple the calculations of the II and IW terms. For small radii, therefore, the IW term was overestimated. For large radii, on the other hand, the II term was underestimated. This made it difficult to obtain reliable results on the basis of the II+IW model.

The above discussion clearly shows the variability of fitting procedures. Therefore, we have been pursuing a theory that is able to explain the molecular mechanisms behind experimental behavior instead of reproduce the experimental data perfectly through fitting.

We think that there is merit in reproducing experimental data (even qualitatively) without adjustable parameters. Our formalism can also provide the individual activity coefficients, γ_i. Our results for γ_i agree with experimental trends too although experiment data are less unambiguous for the individual activity coefficient compared to the mean activity coefficient. These results (to be be reported in a subsequent work) also support the II+IW model.

The success of our approach at low concentrations and its relative inaccuracy at high concentrations reminds us of the limits of the implicit solvent approach. A more comprehensive understanding of the molecular processes governing the behavior of electrolyte solutions can be obtained using explicit water models. Such studies have been available for a while using integral equation theories, particularly, different variations of the reference interaction site model (RISM)[61,79–82]. MD simulation results for structural and solvation properties of electrolyte solutions have also been published[54–60], but free energy calculations are required to obtain the activity coefficients. These are difficult and time consuming simulations using special techniques such as thermodynamic integration. The chemical potential of electrolytes was computed by various workers in studies of solubility of electrolytes[58,83–85]. Moučka and coworkers[86–91] used the Osmotic Ensemble Monte Carlo method to determine the chemical potential. Joung *et al.*[61] used the dielectrically consistent RISM theory and MD simulations to compute the activity coefficient. All these workers used various force fields for water (SPC/E or TIP3P) and ions. The effect of the force fields has been thoroughly studied by Zhang *et al.*[60]. They found that the computed activity coefficients are very sensitive to the chosen force field. This result signifies the main drawback of explicit solvent MD simulations: the force fields are not calibrated thoroughly enough. Another problem is that these simulations are prohibitive for low concentrations. Implicit and explicit solvent approaches, in this respect, complement each other.

Acknowledgments

We acknowledge the support of the Hungarian National Research Fund (OTKA K68641) and the János Bolyai Research Fellowship. Present publication was realized with the support of the project TÁMOP-4.2.2/A-11/1/KONV-2012-0071 and TÁMOP-4.1.1/C-12/1/KONV-2012-0017.

---

[1] F. Malatesta, On the Rodil–Vera method for determining ion activity coefficients, Fluid Phase Equilib. 233 (2005) 103–109.

[2] G. Wilczek-Vera, J. H. Vera, On the measurement of individual ion activities, Fluid Phase Equilib. 236 (2005) 96–110.

[3] G. Wilczek-Vera, E. Rodil, J. H. Vera, A complete discussion of the rationale supporting the experimental determination of individual ionic activities, Fluid Phase Equilib. 244 (2006) 33–45.

[4] G. Wilczek-Vera, J. H. Vera, The activity of individual ions. A conceptual discussion of the relation between the theory and the experimentally measured values, Fluid Phase Equilib. 312

(2011) 79–84.

[5] J. H. Vera, G. Wilczek-Vera, Comment on “The nature of single-ion activity coefficients calculated from potentiometric measurements on cells with liquid junctions” by Dmitri P. Zarubin, J. Chem. Thermodyn. 43 (2011) 1135–1152, J. Chem. Thermodyn. 47 (2012) 442–444.

[6] D. P. Zarubin, Reply to comment by J.H. Vera and G. Wilczek-Vera on ‘The nature of single-ion activity coefficients calculated from potentiometric measurements on cells with liquid junctions’, J. Chem. Thermodyn. 47 (2012) 445–448.

[7] G. Wilczek-Vera, J. H. Vera, Short answer to the reply from D.P. Zarubin to our comment on “The nature of single-ion activity coefficients calculated from potentiometric measurements on cell with liquid-junction”, J. Chem. Thermodyn. 47 (2012) 449–450.

[8] D. P. Zarubin, The debate with G. Wilczek-Vera and J. H. Vera, J. Chem. Thermodyn. 47 (2012) 451–452.

[9] G. Wilczek-Vera, E. Rodil, J. H. Vera, On the activity of ions and the junction potential: revised values for all data, A.I.Ch.E. J. 50 (2004) 445–462.

[10] H. Sakaida, T. Kakiuchi, Determination of Single-Ion Activities of H^+ and Cl^-– in Aqueous Hydrochloric Acid Solutions by Use of an Ionic Liquid Salt Bridge, J. Phys. Chem. B 115 (2011) 13222–13226.

[11] R. A. Robinson, R. H. Stokes, Electrolyte Solutions, 2nd ed., Butterworths, London, 1959.

[12] P. Debye, E. Hückel, The theory of electrolytes. I. Lowering of freezing point and related phenomena, Physik. Z. 24 (1923) 185–206.

[13] J. O. Bockris, A. K. N. Reddy, Modern Electrochemistry, 2nd ed., Plenum Press, New York, 1988.

[14] W. R. Fawcett, Liquids, Solutions, and Interfaces: From Classical Macroscopic Descriptions to Modern Microscopic Details, Topics in Analytical Chemistry, Oxford University Press, New York, 2004.

[15] D. Fraenkel, Simplified electrostatic model for the thermodynamic excess potentials of binary strong electrolyte solutions with size-dissimilar ions, Molec. Phys. 108 (2010) 1435–1466.

[16] D. Fraenkel, Comment on “The nonmonotonic concentration dependence of the mean activity coefficient of electrolytes is a result of a balance between solvation and ion-ion correlations” [J. Chem. Phys. 133, 154507 (2010)], J. Chem. Phys. 134 (2011) 157101.

[17] D. Fraenkel, Monoprotic Mineral Acids Analyzed by the Smaller-Ion Shell Model of Strong

Electrolyte Solutions, J. Phys. Chem. B 115 (2011) 557–568.

[18] D. Fraenkel, Effect of Solvent Permittivity on the Thermodynamic Behavior of HCl Solutions: Analysis Using the Smaller-Ion Shell Model of Strong Electrolytes, J. Phys. Chem. B 115 (2011) 14634–14647.

[19] D. Fraenkel, Single-Ion Activity: Experiment versus Theory, J. Phys. Chem. B 116 (2012) 3603–3612.

[20] D. Fraenkel, Electrolytic Nature of Aqueous Sulfuric Acid. 1. Activity, J. Phys. Chem. B 116 (2012) 11662–11677.

[21] L. Blum, Mean spherical model for asymmetric electrolytes. 1. Method of solution, Mol. Phys. 30 (1975) 1529–1535.

[22] R. Triolo, J. R. Grigera, L. Blum, Simple electrolytes in the mean spherical approximation, J. Phys. Chem. 80 (1976) 1858–1861.

[23] R. Triolo, L. Blum, M. A. Floriano, Simple electrolytes in the mean spherical approximation. III. A workable model for aqueous solutions, J. Chem. Phys. 67 (1977) 5956.

[24] R. Triolo, L. Blum, M. A. Floriano, Simple electrolytes in the mean spherical approximation. 2. Study of a refined model, J. Phys. Chem. 82 (1978) 1368–1370.

[25] J.-F. Lu, Y.-X. Lu, Y.-G. Li, Modification and application of the Mean Spherical Approximation Method, Fluid Phase Equilib. 85 (1993) 81–100.

[26] J.-P. Simonin, L. Blum, P. Turq, Real Ionic Solutions in the Mean Spherical Approximation. 1. Simple Salts in the Primitive Model, J. Phys. Chem. 100 (1996) 7704–7709.

[27] J.-P. Simonin, Real Ionic Solutions in the Mean Spherical Approximation. 2. Pure Strong Electrolytes up to Very High Concentrations, and Mixtures, in the Primitive Model, J. Phys. Chem. B 101 (1997) 4313–4320.

[28] W. R. Fawcett, A. C. Tikanen, Role of Solvent Permittivity in Estimation of Electrolyte Activity Coefficients on the Basis of the Mean Spherical Approximation, J. Phys. Chem. 100 (1996) 4251–4255.

[29] A. C. Tikanen, W. R. Fawcett, Role of Solvent Permittivity in Estimation of Electrolyte Activity Coefficients for Systems with Ion Pairing on the Basis of the Mean Spherical Approximation, Ber. Bunsenges. Phys. Chem. 100 (1996) 634–640.

[30] A. C. Tikanen, W. R. Fawcett, Application of the mean spherical approximation and ion association to describe the activity coefficients of aqueous 1:1 electrolytes, J. Electroanal.

Chem. 439 (1997) 107–113.

[31] G. López-Pérez, D. González-Arjona, M. Molero, Estimation of activity coefficients at different temperatures by using the mean spherical approximation, J. Electroanal. Chem. 480 (2000) 9–17.

[32] Z. Abbas, M. Gunnarsson, E. Ahlberg, S. Nordholm, Corrected Debye-Hückel Analysis of Surface Complexation I. Bulk Salt Limit, J. Coll. Interf. Sci. 243 (2001) 11–30.

[33] Z. Abbas, M. Gunnarsson, E. Ahlberg, S. Nordholm, Corrected Debye-Hückel Theory of Salt Solutions: Size Asymmetry and Effective Diameters, J. Phys. Chem. B 106 (2002) 1403–1420.

[34] M. Gunnarsson, Z. Abbas, E. Ahlberg, S. Nordholm, Corrected Debye-Hückel analysis of surface complexation III. Spherical particle charging including ion condensation, J. Coll. Interf. Sci. 274 (2004) 563–578.

[35] Z. Abbas, E. Ahlberg, S. Nordholm, From restricted towards realistic models of salt solutions: Corrected Debye-Hückel theory and Monte Carlo simulations, Fluid Phase Equilib. 260 (2007) 233–247.

[36] Z. Abbas, E. Ahlberg, S. Nordholm, Monte Carlo Simulations of Salt Solutions: Exploring the Validity of Primitive Models, J. Phys. Chem. B 113 (2009) 5905–5916.

[37] C. W. Outhwaite, M. Molero, L. B. Bhuiyan, Symmetrical Poisson-Boltzmann and modified Poisson-Boltzmann theories, J. Chem. Soc., Faraday Trans. 87 (1991) 3227–3230.

[38] M. Molero, C. W. Outhwaite, L. B. Bhuiyan, Individual ionic activity coefficients from a symmetric Poisson-Boltzmann theory, J. Chem. Soc., Faraday Trans. 88 (1992) 1541–1547.

[39] C. W. Outhwaite, M. Molero, L. B. Bhuiyan, Primitive model electrolytes in the modified Poisson-Boltzmann theory, J. Chem. Soc., Faraday Trans. 89 (1993) 1315–1320.

[40] R. Inchekel, J.-C. de Hemptinne, W. Fürst, The simultaneous representation of dielectric constant, volume and activity coefficients using an electrolyte equation of state, Fluid Phase Equilib. 271 (2008) 19–27.

[41] J. Vincze, M. Valiskó, D. Boda, The nonmonotonic concentration dependence of the mean activity coefficient of electrolytes is a result of a balance between solvation and ion-ion correlations, J. Chem. Phys. 133 (2010) 154507.

[42] J. B. Hasted, D. M. Riston, C. H. Collie, Dielectric properties of aqueous ionic solutions, J. Chem. Phys. (1948) 1–21.

[43] J. B. Hasted, R. G. W., Dielectric properties of aqueous and alcoholic electrolytic solutions, J.

Chem. Phys. 29 (1948) 17–26.

[44] G. H. Haggis, J. B. Hasted, T. J. Buchanan, Dielectric properties of water in solutions, J. Chem. Phys. 20 (1953) 1452–1465.

[45] J. B. Hasted, S. M. El Sabeh, Dielectric properties of water in solutions, Faraday Soc. Trans. 49 (1953) 1003–1011.

[46] K. Giese, U. Kaatze, R. Pottel, Permittivity and dielectric and proton magnetic relaxation of aqueous solutions of the alkali halides, J. Phys. Chem. 74 (1970) 3718–3725.

[47] P. R. Tremaine, S. Goldman, Calculation of Gibbs Free-Energies of Aqueous-Electrolytes to 350 °C from an Electrostatic Model for Ionic Hydration, J. Phys. Chem. 82 (1978) 2317–2321.

[48] H. C. Helgeson, D. H. Kirkham, G. C. Flowers, Theoretical prediction of the thermodynamic behavior of aqueous-electrolytes at high-pressures and temperatures. 4. Calculation of activity-coefficients, osmotic coefficients, and apparent molal and standard and relative partial molal properties to 600 °C and 5 KB, Am. J. Science 281 (1981) 1249–1516.

[49] R. Badarayani, A. Kumar, A simple method to predict the solvation free energy and enthalpy of electrolytes in aqueous and non-aqueous solutions, Indian J. Chem. 39A (2000) 584–588.

[50] N. Gavish, K. Promislow, Dependence of the dielectric constant of electrolyte solutions on ionic concentration, arXiv:01208.5169 (2012).

[51] A. Levy, D. Andelman, H. Orland, Dielectric Constant of Ionic Solutions: A Field-Theory Approach, Phys. Rev. Lett. 108 (2012) 227801.

[52] B. Maribo-Mogensen, G. M. Kontogeorgis, K. Thomsen, Modeling of Dielectric Properties of Complex Fluids with an Equation of State, J. Phys. Chem. B 117 (2013) 3389–3397.

[53] B. Maribo-Mogensen, G. M. Kontogeorgis, K. Thomsen, Modeling of Dielectric Properties of Aqueous Salt Solutions with an Equation of State, J. Phys. Chem. B 117 (2013) 10523–10533.

[54] A. P. Lyubartsev, A. Laaksonen, Calculation of effective interaction potentials from radial distribution functions: A reverse Monte Carlo approach, Phys. Rev. E 52 (1995) 3730–3737.

[55] A. P. Lyubartsev, A. Laaksonen, Concentration Effects in Aqueous NaCl Solutions. A Molecular Dynamics Simulation, J. Phys. Chem. B 100 (1996) 16410–16418.

[56] S. Chowdhuri, A. Chandra, Molecular dynamics simulations of aqueous NaCl and KCl solutions: Effects of ion concentration on the single-particle, pair, and collective dynamical properties of ions and water molecules, J. Chem. Phys. 115 (2001) 3732–3741.

[57] S. Bouazizi, S. Nasr, N. Jaîdane, M.-C. Bellissent-Funel, Local order in aqueous NaCl solutions

and pure water: X-ray scattering and molecular dynamics simulations study, J. Phys. Chem. B 110 (2006) 23515–23523.

[58] E. Sanz, C. Vega, Solubility of KF and NaCl in water by molecular simulation, J. Chem. Phys. 126 (2007) 014507.

[59] A. Savelyev, G. A. Papoian, Molecular Renormalization Group Coarse-Graining of Electrolyte Solutions: Application to Aqueous NaCl and KCl, J. Phys. Chem. B 113 (2009) 7785–7793.

[60] C. Zhang, S. Raugei, B. Eisenberg, P. Carloni, Molecular Dynamics in Physiological Solutions: Force Fields, Alkali Metal Ions, and Ionic Strength, J. Chem. Theor. Comp. 6 (2010) 2167–2175.

[61] I. S. Joung, T. Luchko, D. A. Case, Simple electrolyte solutions: Comparison of DRISM and molecular dynamics results for alkali halide solutions, J. Chem. Phys. 138 (2013) 044103.

[62] R. D. Shannon, C. T. Prewitt, Effective ionic radii in oxides and fluorides, Acta Crystallogr., Sect. B 25 (1969) 925–946.

[63] L. Pauling, The Nature of the Chemical Bond, 3rd ed., Cornell Universiry Press, Ithaca, NY, 1960.

[64] J. Barthel, R. Buchner, M. Münsterer, DECHEMA Chemistry Data Series, volume 12, DECHEMA, Frankfurt a.M., 1995.

[65] R. Buchner, G. T. Hefter, P. M. May, Dielectric Relaxation of Aqueous NaCl Solutions, J. Phys. Chem. A 103 (1999) 1–9.

[66] A. Malasics, D. Boda, An efficient iterative grand canonical Monte Carlo algorithm to determine individual ionic chemical potentials in electrolytes, J. Chem. Phys. 132 (2010) 244103.

[67] A. Malasics, D. Gillespie, D. Boda, Simulating prescribed particle densities in the grand canonical ensemble using iterative algorithms, J. Chem. Phys. 128 (2008) 124102.

[68] M. Born., Volumen und hydratationswarme der ionen, Z. Phys. 1 (1920) 45–48.

[69] J. Barthel, F. Schmithals, H. Behret, Untersuchungen zur Dispersion der komplexen Dielektrizitätskonstante wäßriger und nichtwäßriger Elektrolytlösungen, Z. Phys. Chem. 71 (1970) 115–131.

[70] W. R. Fawcett, Thermodynamic Parameters for the Solvation of Monatomic Ions in Water, J. Phys. Chem. B 103 (1999) 11181–11185.

[71] R. S. Berry, S. A. Rice, J. Ross, Physical Chemistry, 2nd ed., Oxford University Press, New York, 2000.

[72] K. Nörtemann, J. Hilland, U. Kaatze, Dielectric Properties of Aqueous NaCl Solutions at

Microwave Frequencies, J. Phys. Chem. A 101 (1997) 6864–6869.

[73] R. Mancinelli, A. Botti, F. Bruni, M. A. Ricci, A. K. Soper, Hydration of Sodium, Potassium, and Chloride Ions in Solution and the Concept of Structure Maker/Breaker, J. Phys. Chem. B 111 (2007) 13570–13577.

[74] R. Mancinelli, A. Botti, F. Bruni, M. A. Ricci, A. K. Soper, Perturbation of water structure due to monovalent ions in solution, Phys. Chem. Chem. Phys. 9 (2007) 2959–2967.

[75] J. Vincze, M. Valiskó, D. Boda, Response to "Comment on 'The nonmonotonic concentration dependence of the mean activity coefficient of electrolytes is a result of a balance between solvation and ion-ion correlations' [J. Chem. Phys. 134, 157101 (2011)]", J. Chem. Phys. 134 (2011) 157102.

[76] R. Pottel, Dielectric properties, Plenum Press, New York, 1973.

[77] B. Widom, Some Topics in the Theory of Fluids, J. Chem. Phys. 39 (1963) 2808–2812.

[78] B. R. Svensson, C. E. Woodward, Widom's method for uniform and non-uniform electrolyte solutions, Mol. Phys. 64 (1988) 247–259.

[79] B. M. Pettitt, P. J. Rossky, Alkali halides in water: Ion–solvent correlations and ion–ion potentials of mean force at infinite dilution, J. Chem. Phys. 84 (1986) 5836–5844.

[80] J. Perkyns, B. M. Pettitt, A dielectrically consistent interaction site theory for solvent-electrolyte mixtures, Chem. Phys. Lett. 190 (1992) 626–630.

[81] J. Perkyns, B. M. Pettitt, A site–site theory for finite concentration saline solutions, J. Chem. Phys. 97 (1992) 7656–7666.

[82] J. Perkyns, B. M. Pettitt, Integral equation approaches to structure and thermodynamics of aqueous salt solutions, Biophys. Chem. 51 (1994) 129–146.

[83] J. L. Aragones, E. Sanz, C. Vega, Solubility of NaCl in water by molecular simulation revisited, J. Chem. Phys. 136 (2012) 244508.

[84] M. Ferrario, G. Ciccotti, E. Spohr, T. Cartailler, P. Turq, Solubility of KF in water by molecular dynamics using the Kirkwood integration method, J. Chem. Phys. 117 (2002) 4947–4953.

[85] A. S. Paluch, S. Jayaraman, J. K. Shah, E. J. Maginn, A method for computing the solubility limit of solids: Application to sodium chloride in water and alcohols, J. Chem. Phys. 133 (2010) 124504.

[86] M. Lísal, W. R. Smith, J. Kolafa, Molecular Simulations of Aqueous Electrolyte Solubility: 1. The Expanded-Ensemble Osmotic Molecular Dynamics Method for the Solution Phase, J.

Phys. Chem. B 109 (2005) 12956–12965.

[87] F. Moučka, M. Lísal, J. Škvor, J. Jirsák, I. Nezbeda, W. R. Smith, Molecular Simulation of Aqueous Electrolyte Solubility. 2. Osmotic Ensemble Monte Carlo Methodology for Free Energy and Solubility Calculations and Application to NaCl, J. Phys. Chem. B 115 (2011) 7849–7861.

[88] F. Moučka, M. Lísal, W. R. Smith, Molecular simulation of aqueous electrolyte solubility. 3. Alkali-halide salts and their mixtures in water and in hydrochloric acid, J. Phys. Chem. B 116 (2012) 5468–5478.

[89] F. Moučka, I. Nezbeda, W. R. Smith, Molecular simulation of aqueous electrolytes: Water chemical potential results and Gibbs-Duhem equation consistency tests, J. Chem. Phys. 139 (2013) 124505.

[90] F. Moučka, I. Nezbeda, W. R. Smith, Molecular Force Field Development for Aqueous Electrolytes: 1. Incorporating Appropriate Experimental Data and the Inadequacy of Simple Electrolyte Force Fields Based on Lennard-Jones and Point Charge Interactions with Lorentz–Berthelot Rules, J. Chem. Theor. Comp. 9 (2013) 5076–5085.

[91] F. Moučka, I. Nezbeda, W. R. Smith, Molecular force fields for aqueous electrolytes: SPC/E-compatible charged LJ sphere models and their limitations, J. Chem. Phys. 138 (2013) 154102.